Comparison of deck-anchored damper and clipped tuned mass damper on cable vibration reduction

W. J. Wu

Mustang Engineering, 16001 Park Ten Place, Houston, TX, 77084, USA

C. S. Cai[†]

*Department of Civil and Environmental Engineering, Louisiana State University,
Baton Rouge, LA, 70803, USA*

Abstract. Excessive cable vibrations are detrimental to cable-stayed bridges. Increasing the system damping of cables is a key solution to resolve this severe problem. Equations representing the dynamic characteristics of an inclined cable with a Deck-Anchored Damper (DAD) or with a Clipped Tuned Mass Dampers (CTMD) are reviewed. A theoretical comparison on the performance of cable vibration reduction between the cable-DAD system and the cable-CTMD systems is thoroughly discussed. Optimal system modal damping for the free vibration and transfer functions for the forced vibration for the two cable-damper systems are addressed and compared in detail. Design examples for these two different dampers are also provided.

Keywords: cable vibration; TMD damper; viscous damper; system modal damping; transfer function.

1. Introduction

As key load-carrying members of cable-stayed bridges, stay cables are of primary importance to secure the safety of the entire structure. Since cables are generally flexible, relatively light, and low energy-dissipative because of their low intrinsic damping, they are susceptible to external disturbances such as vortex shedding, rain-wind induced vibration, vehicle-induced vibration, and other excitations due to parametric disturbances caused by the motion of the bridge deck and/or towers.

To suppress the problematic cable vibrations, a common practice is to install mechanical dampers at a distance typically 2-5% of the cable span length from the lower end of the cable, with one end of the damper connected to the cable and the other end anchored to the bridge deck. This kind of damper is called deck-anchored damper (DAD) hereafter in this study and its calculation model is shown in Fig. 1(a) that will be discussed later. A lot of research effort has been exerted on DAD system (Pacheco *et al.* 1993, Yu and Xu 1998, Xu and Yu 1998, Main and Jones 2002, Johnson *et al.*

---

† Associate Professor, Corresponding author, E-mail: cscai@lsu.edu

2003). As a device of semi-active control, Magnetorheological (MR) dampers have recently been used as DAD for a few bridges in China because of their advantages over other traditional mechanical dampers, such as the adjustable large damping force, mechanical simplicity, reliability, and minimum power requirement (Chen *et al*. 2003). However, DADs might not be the most effective ones (especially for long cables) because their positions are restricted to the cable end due to the reasons of esthetics and installation issues (Pacheco *et al*. 1993, Cai *et al*. 2007).

To reduce cable vibrations, Tuned Mass Dampers (TMD) was proposed in previous studies where TMDs can be hung anywhere along the cables to overcome the shortcomings of position restriction of the DAD (Tabatabai and Mehrabi 1999). It is well-known that the effectiveness of TMDs depends on and is sensitive to the tuning of the TMD vibration frequency to the cable vibration frequency. In a complicated system it is difficult to predict which mode will be active and what the exact cable vibration frequency is because of the existence of various uncertainties. TMDs with self-adjusting function on its own frequency, such as a TMD-MR damper (Wu and Cai 2006) or other TMDs with variable stiffness will have a broader implementation potential than the traditional TMDs (such as Stockbridge damper). Cai *et al*. (2007) have introduced a MR based TMD that can be clipped anywhere along the cable and can be simplified as a TMD in the calculation model. This clipped TMD is defined as CTMD hereafter in this study and its calculation model is shown in Fig. 1(b) that will be discussed later. They conducted a parametric study on the modal damping of the cable-CTMD system and discussed the influence of different parameters on the effectiveness of the CTMD, represented by the system modal damping.

A comprehensive comparison of the effectiveness of cable vibration reduction between the DAD and CTMD systems is not available in the literature. The current study is to provide some information on this point to aid a deeper understanding of the suitable application conditions for these two types of dampers. Since the out-of-plane vibration of a cable with and without dampers performs the same as a taut cable (Xu and Yu 1998), in this study a comparison in terms of transfer functions and modal damping is focused on the performance of the planar in-plane vibration.

2. Inclined cable with dampers

The present study concerns the planar vibration of an inclined cable with a DAD or CTMD, as shown in Fig. 1. Derivations of both forced vibrations and free vibrations are briefly described below. The former is used to derive the transfer function, while the latter is for the system modal damping.

The viscous DAD is modeled as a dashpot with a damping coefficient C_v anchored to the bridge deck. The DAD is assumed perpendicular to the cable chord for the optimal placement (Xu and Yu 1998). The CTMD (specifically MR-based TMD here) is modeled as an equivalent system consisting of a variable spring K, a dashpot with an adjustable damping coefficient C, and a mass M (Wu and Cai 2006). The damping coefficient C represents the equivalent damping of the MR damper that can be obtained by a linearization process (Li *et al*. 2000). Therefore, the TMD-MR damper is simplified as TMD. Similarly, the CTMD is also perpendicular to the cable chord. As shown in Fig. 1, the damper divides the cable into two segments, with the length indicated in the figure. The notation without subscript will be used to represent either segment and applicable for systems with different dampers. The notation of the cable-DAD system is similar to that of the cable-CTMD damper system, with a subscription of '*v*' to indicate the viscous DAD. The other

(a) Inclined cable with a DAD

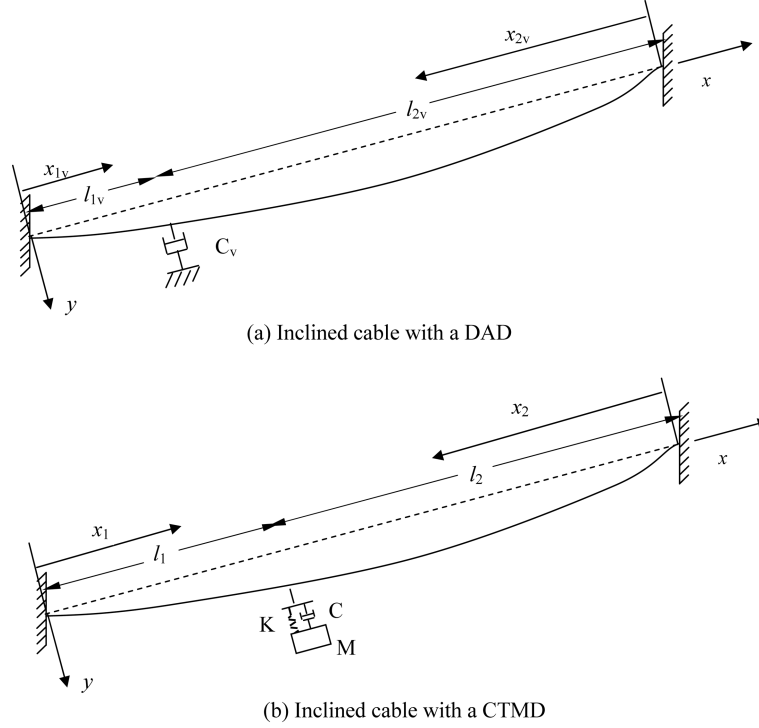(b) Inclined cable with a CTMD

Fig. 1 Calculation model: (a) Inclined cable with a DAD, (b) Inclined cable with a CTMD

notations are self-explaining.

The detailed derivation for such a cable-CTMD configuration was given by Cai *et al.* (2006). The derivation for a cable-DAD configuration can be found in Yu and Xu (1998). However, the important equations and the derivation are summarized here for the convenience of readers. The equation of motion for the cable segment can be expressed as

$$f_y + \frac{H}{\cos\theta}\frac{\partial^2 v}{\partial x^2} + h\frac{d^2 y}{d^2 x} = m\frac{\partial^2 v}{\partial^2 t} + c\frac{\partial v}{\partial t} \tag{1}$$

where f_y is the distributed cable force in the y direction; H is the constant horizontal component of the cable tension force; θ is the inclined cable angle measured from the horizontal axis; v is the cable dynamic displacement component in the y coordinate measured from the static equilibrium position of the cable; m and c are the distributed cable mass and damping coefficient per unit length, respectively; and t is the time. The notation $d(\bullet)/d(\circ)$ and $\partial(\bullet)/\partial(\circ)$ denotes the derivative and partial derivative of "$\bullet$" with respect to "$\circ$", respectively.

A parabolic static profile is chosen by neglecting higher orders of a small quantity ε where $\varepsilon = \frac{mgl}{H}$ $\cos(\theta) << 1$ is the ratio of the cable weight to the tension force. The compatibility equation can be obtained, considering the additional deformation caused by the vibration-induced tension force

$$\frac{h}{EA}\frac{H}{\cos\theta}\left(1 + \frac{1}{8}\varepsilon^2\cos^2\theta\right)l = \varepsilon\cos\theta\int_0^l v\,dx \tag{2}$$

where E is the Young's modulus of the cable; A is the area of the cable cross section; and h is

defined as the component of the dynamic tension force along the x ordinate.

The cable equation can be analytically solved for some specific loadings such as $f_y = \tilde{f}_y(x)e^{st}$, leading to the following solution

$$\tilde{v}_k(x) = \tilde{v}_d \frac{\sinh(\beta x)}{\sinh(\beta l_k)} - \left(\frac{\tilde{f}_y l - \tilde{h}\varepsilon\cos(\theta)}{\beta^2 l}\right)\left(\frac{\sinh(\beta(l_k - x)) + \sinh(\beta x)}{\sinh(\beta l_k)} - 1\right), \quad k = 1, 2 \qquad (3)$$

where v_d is the cable displacement where the damper is located and β is defined as $\sqrt{(ms^2 + cs)}\cos(\theta)/H$. $k = 1, 2$ indicates the cable segment number shown in Fig. 1. The complex variable s can be viewed similar to an angular frequency, which represents the vibration characteristics. Terms with a tilde represent that they are functions of the position only.

The damper provides a damping force to the cable, which can be expressed in Eqs. (4) and (5) for a DAD and a CTMD, respectively,

$$\frac{H}{\cos\theta}\left(-\frac{\partial v_{1v}}{\partial x_1}\bigg|_{x_1 = l_{1v}} - \frac{\partial v_{2v}}{\partial x_2}\bigg|_{x_2 = l_{2v}}\right) = C_v \frac{\partial v_c}{\partial t} \qquad (4)$$

$$\frac{H}{\cos\theta}\left(-\frac{\partial v_1}{\partial x_1}\bigg|_{x_1 = l_1} - \frac{\partial v_2}{\partial x_2}\bigg|_{x_2 = l_2}\right) = K(v_1|_{x_1 = l_1} - v_d) + C\left(\frac{dv_1}{dt}\bigg|_{x_1 = l_1} - \frac{dv_d}{dt}\right) \qquad (5)$$

The equilibrium of the CTMD itself should also be counted in, as

$$K(v_1|_{x_1 = l_1} - v_d) + C\left(\frac{dv_1}{dt}\bigg|_{x_1 = l_1} - \frac{dv_d}{dt}\right) - M\frac{d^2 v_d}{dt^2} = 0 \qquad (6)$$

With further derivation from the previous simultaneous equations, the eigenvalue equation governing the free vibration problem of the cable-DAD system can be obtained from Eqs. (2)-(4) with $\tilde{f}_y = 0$ as

$$4\pi\xi\sinh(\beta' r_{1v})\sinh(\beta' r_{2v})\left\{\sinh(\beta') - \cosh(\beta' r_{1v})\cosh(\beta' r_{2v})\left(\beta' + \frac{4}{\lambda^2}\beta'^3\right)\right\}$$

$$= -\sinh(\beta')\left\{\sinh(\beta') - \cosh(\beta')\left(\beta' + \frac{4}{\lambda^2}\beta'^3\right)\right\} \qquad (7)$$

where $r_{1v} = l_{1v}/l, r_{2v} = l_{2v}/l$, $\beta' = 0.5\beta l$, and $\xi = C_v/(2ml\omega_0)$. $\omega_0 = \sqrt{H/m\cos\theta}\,\pi/l$ is the fundamental angular frequency for a taut cable, and λ^2 is proportional to the ratio of the cable axial stiffness to the cable geometry stiffness and thus called the cable geometry-elasticity parameter hereafter

$$\lambda^2 = \varepsilon^2\cos^2(\theta)\frac{1}{1 + \frac{1}{8}\varepsilon^2\cos^2\theta}\frac{AE}{H/\cos\theta} \qquad (8)$$

Similarly, the governing equation for the free vibration problem of the cable-CTMD system can be obtained from Eqs. (2), (3), (5), and (6) with $\tilde{f}_y = 0$ as

$$4m_r\beta'\frac{\rho^2+4\eta\rho(\beta'/\pi)}{\rho^2+4\eta\rho(\beta'/\pi)+4(\beta'/\pi)^2}\sinh(\beta'r_1)\sinh(\beta'r_2)$$

$$\left\{\sinh(\beta')-\cosh(\beta'r_1)\cosh(\beta'r_2)\left(\beta'+\frac{4}{\lambda^2}\beta'^3\right)\right\}=-\sinh(\beta')\left\{\sinh(\beta')-\cosh(\beta')\left(\beta'+\frac{4}{\lambda^2}\beta'^3\right)\right\} \quad (9)$$

where $m_r = M/ml$ is the mass ratio between the CTMD, η is the damper damping ratio, and the cable and ρ is the frequency ratio of the CTMD and the taut cable, and simply called frequency ratio hereafter.

The simultaneous equations for the cable-DAD system on the forced vibration problem with an evenly distributed force in the form of $f_y = \tilde{f}_y(x)e^{st}$ are listed below, which can be obtained from Eqs. (2)-(4).

$$\tilde{v}_c\left(2\pi\xi+\frac{\sinh(\beta')}{\sinh(\beta'r_1)\sinh(\beta'r_2)}\right)+\frac{\tilde{h}\varepsilon\cos^2\theta}{H\beta^2l}\times\frac{\sinh(\beta'/2)}{\cosh(\beta'r_1/2)\cosh(\beta'r_2/2)}$$

$$=\frac{\tilde{f}_y\cos\theta}{\beta^2H}\times\frac{\sinh(\beta'/2)}{\cosh(\beta'r_1/2)\cosh(\beta'r_2/2)} \quad (10\text{-a})$$

$$\tilde{v}_c\times\frac{\sinh(\beta'/2)}{\cosh(\beta'r_1/2)\cosh(\beta'r_2/2)}+\frac{\tilde{h}\varepsilon\cos^2\theta}{H\beta^2l}\left(\frac{2\sinh(\beta'/2)}{\cosh(\beta'r_1/2)\cosh(\beta'r_2/2)}-\beta-\frac{\beta^3}{\lambda^2}\right)$$

$$=\frac{\tilde{f}_y\cos\theta}{\beta^2H}\left(\frac{2\sinh(\beta'/2)}{\cosh(\beta'r_1/2)\cosh(\beta'r_2/2)}-\beta\right) \quad (10\text{-b})$$

Similarly, the equations for the forced vibration of the cable-CTMD system can be found in Cai *et al.* (2006), or simply by changing the term $2\pi\xi$ in Eq. (10-a) to the corresponding term for the CTMD damper.

3. Comparison on achievable system modal damping

The first five modal damping is compared between the cable-DAD system and the cable-CTMD system. Note that since the installation of the CTMD damper adds one more degree of freedom to the cable-CTMD system (i.e., one mode splits into two modes), only the cable related mode is compared. The cable related mode is defined as the one with a smaller ratio of the CTMD modal amplitude and the cable modal amplitude at the damper location. The other mode is defined as the damper related mode or the zero-th mode since it is an extra mode due to the addition of the CTMD. Both modes have equal importance for the cable-CTMD system (Wu and Cai 2006).

Irvine (1981) predicted that the nth frequency crossover occurs when the cable geometry-elasticity parameter λ^2 reaches $(2\pi n)^2$ for a horizontal cable. Triantafyllou (1984) held the opinion that a frequency-avoidance replaces the frequency crossover when the geometry-elasticity parameter λ^2 is equal to $(2\pi n)^2$ for an inclined cable. Cables with different λ^2 values are considered in this study by varying the cable forces to investigate the damper performance with different λ^2. These considered λ^2 values are: 0.012, 6.19, 39.88, and 49.54 that corresponds to far less than, less than, close to, and larger than the first frequency crossover point $(2\pi)^2 = 39.48$.

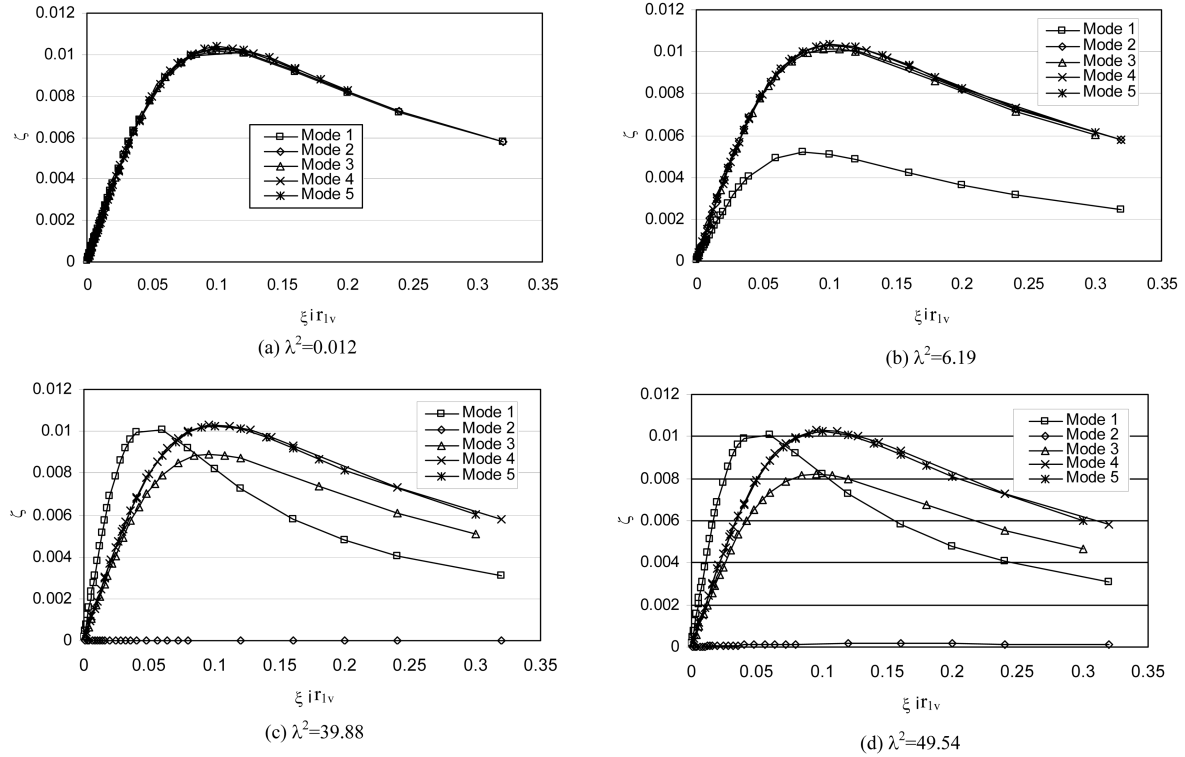Though a DAD can perform better when its location moves toward the mid-span, a damper

Fig. 2 Variations of system modal damping with DAD damping (r_1=0.02): (a) λ^2 = 0.012, (b) λ^2 = 6.19, (c) λ^2 = 39.88, (d) λ^2 = 49.54.

position more than 5% of the cable length away from the cable end is deemed impractical. Therefore, only two damper locations, $0.02l$ and $0.05l$ from the lower cable end, are considered to reveal the variation trends of the system damping due to the change of the geometry-elasticity parameter λ^2, the damper location r_{1v}, and the damping ratio ξ. The mass ratio m_r for the cable-CTMD system is chosen as 0.02, as commonly used in practice for TMD type of device. The tuning of the CTMD frequency to that of the cable is chosen as $\omega_d/\omega_{c1} = 1$, where the ω_d and ω_{c1} are the CTMD frequency and the cable fundamental frequency, respectively.

Fig. 2 displays the relationship between the normalized damper damping ratio and the system modal damping for the cable-DAD systems with four different λ^2 values discussed earlier. The damper is placed at $0.02l$ from the lower cable end. Figs. 2(a) and 2(b) are similar to Pacheco's results (Pacheco *et al*. 1993). Fig. 2(a) shows the so-called universal modal damping curves. It can be seen that for a cable with a small λ^2 value (corresponding to a very large tension force in the cable), when the system modal damping is plotted against $\xi i r_{1v}$, i.e., the multiplication of the damper damping ratio ξ, the mode number i, and the damper location parameter r_{1v}, the curves for the first five modes are very close. Fig. 2(b) shows that when the λ^2 value increases due to the decrease of the cable force, the curve for the first modal damping moves down. However, the other four modal damping curves almost do not change.

With a further increase of the λ^2 value to 39.88 that is slightly larger than the first frequency crossover point (39.48), several modal damping curves are considerably affected as shown in
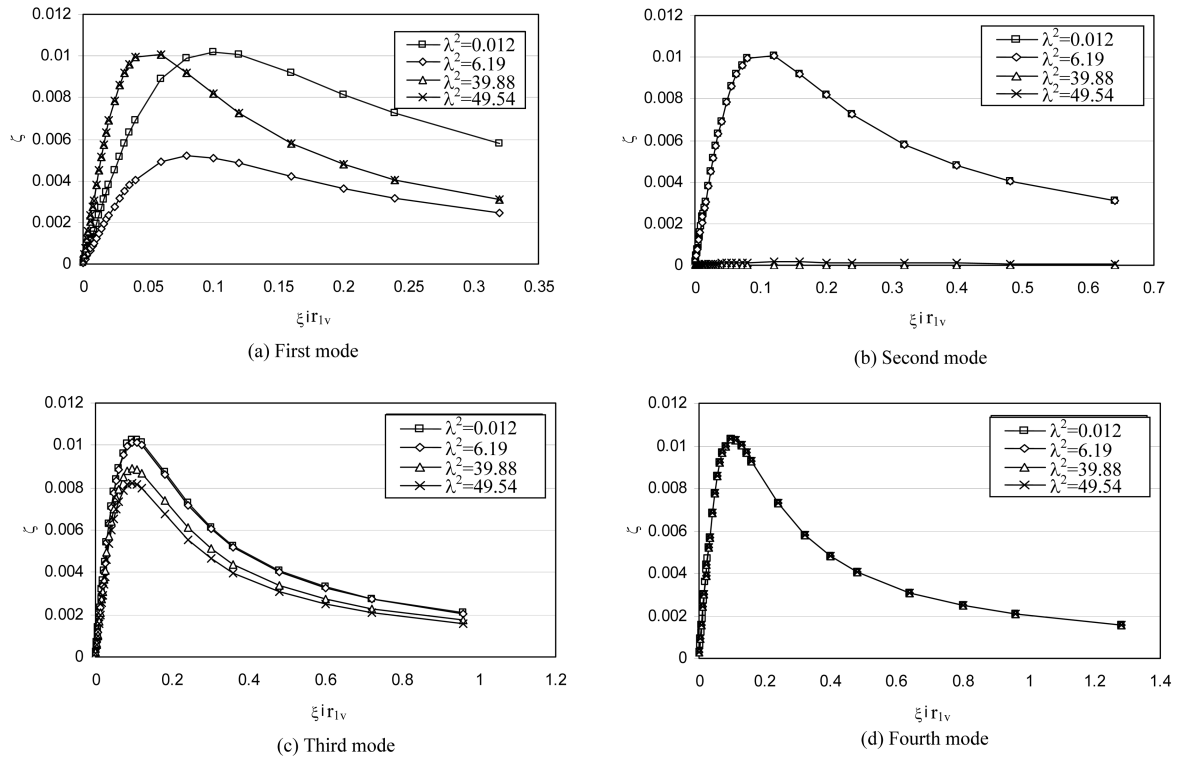
Fig. 3 Variations of system modal damping with DAD damping ($r_1 = 0.02$): (a) first mode, (b) second mode, (c) third mode, (d) fourth mode

Fig. 2(c). The first modal damping curve ascends back to the same level as in Fig. 2(a) with the optimal damping ratio shifting towards the left in the x-axis. The second modal damping curve becomes close to zero, and the third modal damping curve drops down. With a further increase of the λ^2 value to 49.54 in Fig. 2(d), the second modal damping curve begins to rise a little bit, the third modal damping curve lowers down more, and the other curves remain without noticeable change.

Fig. 3 shows the change of the modal damping curves affected by the geometry-elasticity parameter for each mode. In Fig. 3(a) the first modal damping curve decreases when the λ^2 value increases from 0.012 (a taut cable) to 6.19. After it reaches 39.88 that is beyond the first frequency crossover point (39.48), the modal damping comes back almost to the same optimal modal damping level of a taut cable, and remains unchanged afterwards for a further increase of λ^2 to 49.54. In Fig. 3(b) the second modal damping curve stays unvaried before the λ^2 value reaches the first frequency crossover point (λ^2 changes from 0.012 to 6.19), becomes zero at the crossover point. In Fig. 3(c) the third modal damping curve continues to decrease when the λ^2 value increases while in Fig. 3(d) the fourth modal damping curve does not vary much, when the λ^2 value changes in the considered range.

These observations can be explained with the mode exchange rule occurred at the frequency crossover point. Irvine (1981) pointed out that at the first frequency crossover point, the first and second modes exchange. As Xu and Yu (1998) discussed, before the frequency crossover occurs the
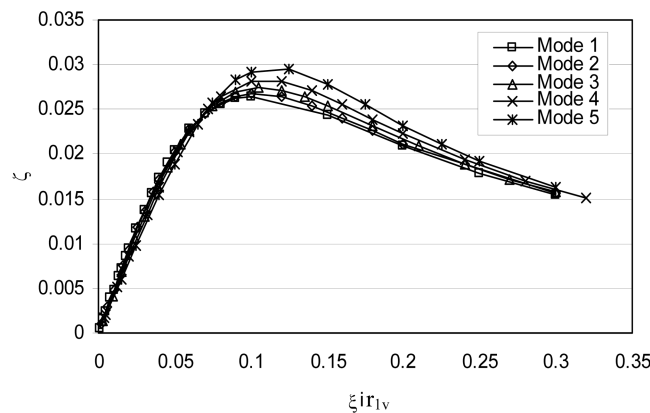
Fig. 4 The modal damping for a DAD at $r_1 = 0.05$ with $\lambda^2 = 0.012$

modal shape ordinate close to the cable end of the first symmetric mode entails for the cable a very small motion over there, thus causing a small first modal damping. However, after the frequency crossover occurs, the first and second mode exchange occurs and all the mode-related properties exchange accordingly. Therefore, the descending first modal damping curve rises back to the original height (the first mode becomes the second one), and the unmoved second modal damping curve drops dramatically at that point (the second mode becomes the first one). Since the λ^2 value considered is far below the second frequency crossover point, there is no mode exchange between the modes 3 and 4 and the fourth modal damping curve is not influenced by the considered λ^2 values.

Presented in Fig. 4 is the variation of the system modal damping versus the DAD damping ratio when the damper is located at the $0.05l$ from the cable end, while the λ^2 value (0.012) is the same as in Fig. 2(a). The maximum modal damping in Fig. 4 increases from 0.01 in Fig. 2(a) to around 0.025-0.03 in this figure, which is not proportional to the damper location as observed in the universal curve (Pacheco 1993). The five curves separate and the higher modes attain larger optimal system modal damping while in Fig. 2(a), they overlap each other and have the same universal damping curve. Therefore, the universal modal damping curve is only eligible for the design of DADs located very close to the cable end to mitigate cable vibration with a small λ^2 value. In other words, the curves may not be universal any more once the damper moves more towards the mid-span. The comparison results for the damper located at $0.02l$ and $0.05l$ for cables with other λ^2 values are similar and therefore, are not shown here.

Fig. 5 shows the relationship between the system modal damping and the CTMD damping ratio for the cable-CTMD system for four different λ^2 values discussed earlier with a damper location parameter $r_1 = 0.25$, i.e., at quarter span (There is no position restriction for CTMD). The modal damping curve of the damper related mode is not plotted because it cannot fit nicely in the figure due to its too large value compared with the others. All five curves separate from each other in Fig. 5(a), unlike Fig. 2(a). With the CTMD frequency turned to the first mode, the peak modal damping for the first mode achieved by the CTMD is almost 5 times of that achieved by the DAD, as shown in Fig. 2(a). Actually, over a large range of damper damping ratio η, the cable-CTMD system has achieved a higher system modal damping than the cable-DAD system located at either $0.02l$ or $0.05l$ from the cable end. Even the modal damping of the second mode for the cable-CTMD system is larger than the maximum modal damping of the cable-DAD system shown in
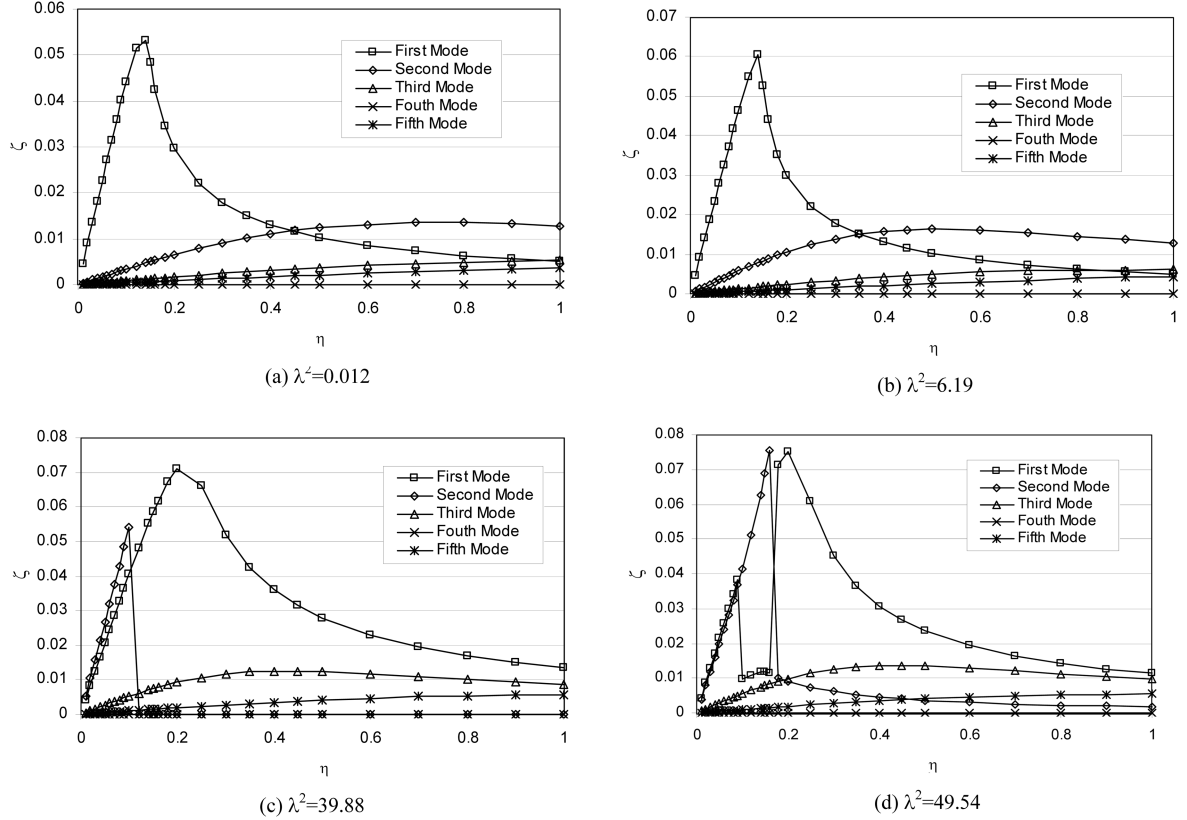
Fig. 5 Variations of modal damping with the damping ratio of a CTMD for four cables: (a) $\lambda^2 = 0.012$, (b) $\lambda^2 = 6.19$, (c) $\lambda^2 = 39.88$, (d) $\lambda^2 = 49.54$

Fig. 2(a) for a considerable range.

However, the peak modal damping for the cable-DAD system is less sensitive in terms of the damper coefficient compared to the cable-CTMD system. The half-value bandwidth of the damper coefficient is defined for this comparison. If C_a and C_b (or their proportional counterparts) are the damper coefficients that correspond to the two points where the amplitude of the modal damping ζ is half of the peak modal damping, then the magnitude of the term $|C_b - C_a|$ is defined as the half-value bandwidth of the damper coefficient. This concept can be used to check the sensitivity of the optimal damper damping coefficient. The half-value bandwidth calculated from the first modal damping curve for the DAD is about 11288 N.s/m, while it is 2.26 N.s/m for the CTMD damper. This indicates that though the CTMD damper can provide better performance and save material, it needs a more accurate design since it has a narrower half-value bandwidth.

As shown in Fig. 5, when the λ^2 value increases, the maximum first modal damping of the cable-CTMD system increases, indicating that CTMD can provide more damping for flexible cables, which is opposite to that of the cable-DAD system, as shown in Fig. 3(a). The half-value bandwidth of the first modal damping curve increases from 2.26 to 4.37 N.s/m for the cable-CTMD system when the λ^2 value increases from 0.012 to 39.88, as shown in Fig. 5(c). However, the half-value bandwidth for the cable-DAD system decreases from 11288 N.s/m to 5855 N.s/m, as shown in Fig. 3(a).

Fig. 5(c) also shows the effect of the mode exchange on the system modal damping. When the CTMD damping ratio reaches a certain value (0.1 in this case), mode exchange occurs between the second and zero-th modes. After the mode exchange, the second modal damping becomes zero, while the zero-th modal damping continues the track for the second mode (not shown since it cannot be fit nicely in this figure).

Actually, at the vicinity of the frequency crossover point, there is a complex interaction between the first two cable frequencies and the damper frequency tuned to the first cable mode. Near the frequency crossover point, the three frequencies are so close that either two of them may exchange. A more complicated mode exchange phenomenon occurs in Fig. 5(d). Therefore, cables with λ^2 value close to the frequency crossover point are not recommended because of the uncertainty and unpredictability. In this range, neither the DAD nor the CTMD damper can guarantee a good performance in a predictable way. In practice, 90% of the stay cables have a λ^2 value in the range of 0.008-1.08 based on the database of stay cables established by Tabatabai *et al.* (1998), which are far less than the frequency crossover point ($\lambda^2 = 39.48$).

The third modal damping curve increases slowly when the λ^2 value increases and is much lower compared to the first two modal damping curves. The fourth system modal damping curve is always zero since the quarter-span length point where the CTMD is located is a node for the fourth mode.

4. Comparison on transfer function

To evaluate the performance of the dampers, in addition to the system modal damping based on free vibrations, the reduction of the cable resonant response to forced vibrations is also investigated. In the current study, mitigation of the first modal vibration is considered. Since cables with geometry-elasticity parameters close to and larger than the frequency crossover point are not recommended as discussed earlier, the cable with only two λ^2 values (0.012 and 6.19) less than the first frequency crossover point are considered in this section. A small distributed damping c of 0.493 N.s/m^2 for the cable is chosen for the pure cable without dampers to avoid the divergent resonant response.

Pacheco *et al.* (193) and Xu and Yu (1998) pointed out that a viscous DAD provides more achievable damping for the cable-damper system for the first five modes when the damper location moves toward the mid-span (This is also observed by comparing Fig. 2(a) and Fig. 4 in this paper). The damper location considered in their study is up to 0.10l from the lower cable end, which is beyond the implementation restriction and more of theoretical interest. Therefore, the optimal location in the current study for a viscous DAD is selected as a practical 0.05l, perhaps the furthest practically possible location in applications. The viscous DAD that can provide maximum modal damping for a free vibration may not be exactly the same one to achieve the best forced vibration reduction, but they should be close. Therefore, the optimal viscous DAD for the free vibration is taken as the initial guess and may be updated if a better one is found using a search step of 0.01 of the damper damping ratio in its vicinity.

For the CTMD damper, the optimal tuning frequency is obtained by a trial-and-error process with a 0.01 step length of the tuning ratio (the CTMD frequency to the fundamental cable frequency ω_d/ω_{c1}) and the same step size for the damper damping ratio η. The mass ratio of the CTMD damper to the cable is chosen as 0.02. Two different CTMD damper locations, i.e., at the mid-span and quarter-span cable length, are chosen to achieve a best first modal reduction and an overall

(a) CTMD damper at mid-span   (b) CTMD damper at quarter-span cable length
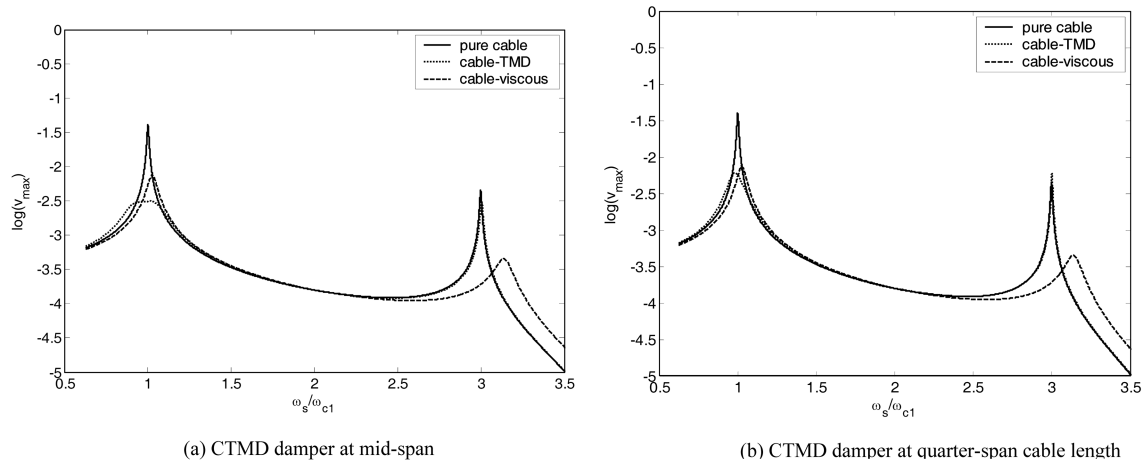
Fig. 6 Transfer function comparison: (a) CTMD damper at mid-span, (b) CTMD damper at quarter-span cable length

Table 1 Comparison of cable vibration reduction between DAD and CTMD for the first mode

Cable	CTMD location	CTMD			DAD $r_1 = 0.05$	
		Damping ratio (η)	Tuning frequency (ω_d/ω_{c1})	Optimal reduction (r_{red})	Damping ratio (ξ)	Optimal reduction (r_{red})
$\lambda^2 = 0.012$	Mid-span	0.15	0.96	0.0776	1.05	0.185
	Quarter-span	0.15	1.00	0.1495		
$\lambda^2 = 6.19$	Mid-span	0.17	0.96	0.0677	0.85	0.2936
	Quarter-span	0.15	1.01	0.1259		

reduction for all modes, separately.

Fig. 6(a) shows the transfer function for the pure cable and the cable with dampers for the case of $\lambda^2 = 0.012$. There is no peak response associated with the second cable mode in this figure (near $W_s/W_{cl} = 2$) since it cannot be excited by the evenly distributed force. The optimal damper damping ratio for the DAD is $\xi = 1.05$ and a reduction ratio of $r_{red} = 0.185$ that is defined as the ratio of the maximum displacement at the middle point of the cable with the damper to that without the damper. The optimal reduction ratio for the cable-CTMD damper system is achieved as $r_{red} = 0.0776$ with a tuning ratio of $\omega_d/\omega_{c1} = 0.96$ and a damper damping ratio of $\eta = 0.15$. In this case the two supposed peaks for the cable-CTMD damper system are close, and thus appear like one with a broader range (near $W_s/W_{cl} = 1$). Therefore, the optimal vibration by installing the CTMD damper is another 58.1% less than that by using the DAD. For the third mode, (near $W_s/W_{cl} = 3$) the DAD provides a much better reduction than the CTMD damper since only the first mode is targeted in the CTMD tuning design. Since the vibration of the third mode is already very small, it is not important to reduce this vibration. The comparison for the CTMD damper at the quarter-span of the cable length and the DAD is similar and is shown in Fig. 5(b). Data for both cases are summarized in Table 1. The comparison results for the cable with a λ^2 value of 6.19 are similar to that with a λ^2 value of 0.012, which are also summarized in Table 1.

Table 2 Properties of the example cable

m (kg·m^{-1})	l (m)	T (N)	p (kg/m^3)	D (m)	ω_{c1} (sec^{-1})
114.09	93	$5.017*10^6$	1.29	0.225	7.08

5. Comparison of damper design

The design of viscous DAD for a taut cable using a universal damping curve was proposed by Pacheco *et al.* (1993). A similar approach of a CTMD damper design for cables can be found in Wu and Cai (2006). A brief summary and comparison between the designs of these two dampers for a taut cable are introduced here for demonstration purposes, based on the example used by Wu and Cai (2006). Assuming that the intrinsic cable damping is conservatively ignored and additional damping is needed to suppress the so-called rain-wind induced cable vibrations that have become serious for many cable-stayed bridges. Other cable properties are listed in Table 2. Damper designs for cables with larger λ^2 values need more information and effort, but they can follow the same procedure.

Irwin (1997) proposed the following criterion to control the rain-wind induced cable vibrations

$$S_c = \frac{m\zeta}{\rho D^2} \geq \alpha \tag{11}$$

where S_c is the Scruton number; ρ is the mass density of air; D is the outside diameter of the cable; and α is the limiting value for Scruton number. The above relationship can be rewritten as

$$\zeta \geq \frac{\alpha \rho D^2}{m} = \frac{\alpha}{\mu} \tag{12}$$

where the mass parameter μ is defined as $\mu = m/(\rho D^2)$. Therefore, to meet the above stated criterion, the damping ratio of the cable needs to meet the requirement of Eq. (12). Based on available test results, Irwin proposed a minimum α value of 10.

Since the mass parameter μ can be calculated as $\mu = m/(\rho D^2) = 1747$, the demanded system modal damping is determined from Eq. (12) as

$$\zeta_1 \geq \alpha/\mu = 10/1747 = 0.0057 = 0.57\% \tag{13}$$

5.1 Design of viscous DAD

To design a viscous DAD located at $0.02l$, the damper coefficient of the viscous DAD can be designed using Fig. 2(a). Based on this figure, values of ξir_{1v} from 0.032 to 0.32 (from that the corresponding ξ can be calculated) will satisfy Eq. (13) and the corresponding damper coefficient is calculated as

$$Cv = 2mlw_0\xi = 2 \times 114.09 \times 93 \times 7.08 \times \xi = 240388 \text{ to } 2403885 \text{ N.s/m} \tag{14}$$

The optimal DAD damping coefficient that corresponds to the maximum system modal damping ratio is obtained as 901457 N.s/m that falls in the feasible range 240388 to 2403885 N.s/m.

5.2 Design of CTMD

Suppose the CTMD is placed at the quarter-span cable length. The mass ratio of the CTMD chosen as 2% as in common practice, from which the mass of the damper is determined as

$$M = 2\% \times l \times m = 0.02 \times 93 \times 114.09 = 212.2 \text{ kg} \tag{15}$$

The frequency tuning ratio is then chosen approximately as $\omega_d/\omega_{c1} = 1.0$ for simplicity, though a optimal tuning may achieve a little bit higher system modal damping. The stiffness of the CTMD damper can thus be determined as

$$K = M\left(\frac{\pi}{l}\sqrt{\frac{T}{m}}\right)^2 = 212.2 \times \left(\frac{3.14159}{93}\sqrt{\frac{5.017 \times 10^6}{114.09}}\right)^2 = 10648.2 \text{ N/m} \tag{16}$$

where $\omega_{c1} = \pi/l\sqrt{T/m}$ is the fundamental frequency for a taut cable. Then Fig. 5(a) can be referred to and $\eta = 0.012$ to 0.83 can be chosen to satisfy Eq. (13) with an optimal damping ratio at 0.14, which corresponds to a damper coefficient of 420.7 N.s/m.

From the procedure stated above, the design effort is similar for these two dampers. The damping required for the cable-CTMD system is less than that for the cable-DAD system. Therefore, to achieve the same system modal damping for the fist mode, the damper required for the CTMD system is smaller than that for the DAD system. However, as discussed earlier, the DAD can cover wide frequency range.

6. Conclusions

A comparative study between the characteristics of the cable-DAD system and the cable-CTMD system is presented through an analytical approach. From this study, the following conclusions can be drawn:

1. The system modal damping depends on the cable geometry-elasticity parameter λ^2 for both the cable-DAD system and the cable-CTMD damper system. For both systems, modal exchange occurs at the frequency crossover point and the modal performance becomes sensitive and unpredictable. However, actual cables of cable-stayed bridges are far away from the condition of frequency crossover; thus frequency crossover is not a concern for cable-stayed bridges.

2. For the comparison between an optimal viscous DAD located at 0.05*l* from the cable end and an optimal CTMD damper located at quarter-span cable length or mid-span with a 0.02 mass ratio, the CTMD damper can provide better vibration reduction to the targeted first mode and needs a smaller damper. However, it needs a more accurate design since its reduction effect is more sensitive to the damper's damping ratio.

3. The viscous DAD is effective for more modes at the same time, while the CTMD damper is more focused to the targeted mode. It may need multiple CTMD dampers to reduce vibrations for several modes.

4. The design procedure to mitigate the rain-wind induced cable vibration with a viscous DAD and a CTMD damper are similar. All the damper parameters can be obtained according to the demanded system modal damping calculated based on the Scruton number requirement.

References

Cai, C.S., Wu, W.J. and Araujo, M. (2007), "Cable vibration control with a TMD-MR damper system: experimental exploration", *J. Struct. Eng.*, ASCE, **133**(5), 629-637.

Cai, C.S., Wu, W.J. and Shi, X.M. (2006), "Cable vibration reduction with a hung-on TMD system I: Theoretical study", *J. Vib. Control.*, **12**(7), 801-814.

Chen, Z.Q., Wang, X.Y., Ko, J.M., Ni, Y.Q., Spencer, B.F. and Yang, G.Q. (2003), "MR damping system on Dongting Lake cable-stayed bridge", *Smart Systems and Nondestructive Evaluation for Civil Infrastructures*, San Diego, California, USA, 2-6 March 20.

Irvine, H.M. (1981), "Cable structure", MIT Press Series in Structural Mechanics, Cambridge, Massachusetts, and London, England, 1981.

Irwin, P.A. (1997), "Wind vibration of cables on cable-stayed bridges", *Proceedings of Structural Congress*, ASCE, New York, 383-387.

Johnson, E.A., Christenson, R.E. and Spencer, B.F. Jr. (2003), "Semiactive damping of cables with sag", *Comput-Aided Civ. Inf.*, **18**, 132-146.

Li, W.H., Yao, G.Z., Chen, G., Yeo, S.H. and Yap, F.F. (2000), "Testing and steady state modelling of a linear MR damper under sinusoidal loading", *Smart Mater. Struct.*, **9**, 95-102.

Main, J.A. and Jones, N.P. (2002), "Free vibrations of taut cable with attached damper. I: Linear viscous damper", *J. Eng. Mech.*, **128**(10), 1062-1071.

Pacheco, B.M., Fujino, Y. and Sulekh, A. (1993), "Estimation curve for modal damping in stay cables with viscous damper", *J. Struct. Eng.*, **119**(6), 1961-1979.

Stockbridge damper. "http://www.dulhunty.com/an3.htm."

Tabatabai, H. and Mehrabi, A.B. (1999), "Tuned dampers and cable fillers for suppression of bridge stay cable vibrations", IDEA Program Final Report, Construction Technology Laboratories, Inc., Skokie, IL.

Tabatabai, H., Mehrabi, A.B., Morgan, B.J. and Lotfi, H.R. (1998), "Non-destructive bridge technology: Bridge stay cable condition assessment", Final report submitted to the Federal Highway Administration, Construction Technology Laboratories, Inc., Skokie, IL.

Triantafyllou, M.S. (1984), "The dynamics of Taut inclined cables", *Quarterly J. Mech. Appl. Math.*, **27**(3), 421-440.

Wu, W.J. and Cai C.S. (2006), "Cable vibration reduction with a hung-on TMD system II: Parametric study", *J. Vib. Control.*, **12**(8), 881-899.

Xu, Y.L. and Yu, Z. (1998), "Mitigation of three dimensional of inclined sag cable using discrete oil dampers-II. application", *J. Sound Vib.*, **214**(4), 675-693.

Yu, Z. and Xu, Y.L. (1998), "Mitigation of three dimensional vibration of inclined sag cable using discrete oil dampers-I. formulation", *J. Sound Vib.*, **214**(4), 659-673.